Continuous Triple Log Gaussian Dark Current in 3-Tap Indirect ToF Sensors

Takahiro Akutsu, Masanori Nagase and Takashi Watanabe

Brookman Technology, Inc., 125 Daikumachi, Naka-ku, Hamamatsu, 430-0936 Japan

Contact: Takahiro Akutsu: phone:+81-53-482-7570, E-mail: t_akutsu@brookmantech.com

ABSTRACT

In this paper, we present two observed facts on the Floating Diffusion’s (FD’s) dark current in 3-Tap Indirect Time-of-Flight sensors (3T_iToF). The first is that the dark current is generated by three dominant causes, and the second is that those causes correspond to the continuous log Gaussian model.

INTRODUCTION

Time-of-Flight (ToF) sensors have been in growing demand for 3D sensing such as robotics, mobility, drone, monitoring, VR/AR/MR, medical, gesture, face recognition, and gaming. We’ve been developing a FD storage 3T_iToF for several years.

In the 3T_iToF, photodiode (PD) charges of all pixels are transferred and integrated into 3-Tap FDs in each pixel. Thus, FD’s dark current gives a serious impact on the performance of the 3T_iToF. For this reason, it is important to understand the FD's dark current behavior [1].

Many studies on the dark current of FD (N+ diffusion) have been reported. For instance, it is known that the FD dark current is approximated by a Log Gaussian model [2], and the large potential difference gap between gate and drain causes a large dark current by the Gate Induced Leakage Trap Assisted Tunneling (GIL-TAT) mechanism [3][4][5][6].

In this paper, we introduce that the two observed facts on the FD’s dark current in 3T_iToF. The first is that the FD dark current is generated by three dominant causes, which correspond to the Triple Log Gaussian (TLG) model. The second is that these are explained by TAT, Shockley Read Hall (SRH) and Diffusion mechanisms, and the distributions of these mechanisms are continuous.

METHOD AND ANALYSIS

Figure 1 shows a 3T_iToF pixel circuit. In this 3T_iToF, three transfer gates (G1, G2, and G3) distributes PD charges to each FD with a MOS capacitor [1]. Distributed PD charges are integrated into each FD.

Figure 2 and Figure 3 show the FD’s dark current histogram and the log cumulative probability plot [7], respectively. The total pixel number is 310k. Figure 3 indicates three distributions shown by (i), (ii), and (iii), whose trends are different. In other words, it indicates a TLG model. According to the temperature dependency of the TLGs in Figure 3, this result implies that the mechanism of dominant dark current generation is different. To identify the mechanism, an activation energy (Ea) in pixel-level was calculated from the Arrhenius plot using the observed data at 60℃, 70℃, and 80℃.

Figure 4 and Figure 5 show the Ea histogram of all pixels and the cumulative probability plot [8], respectively. As shown in Figure 5, three Ea distributions of (A), (B), and (C) are found. This fact indicates the dark current is generated by the three dominant causes, and these distributions are continuous.

Figure 6 shows the scatter plot of Ea versus dark current for all pixels, and Figure 7 shows the 3D plots of dark current and Ea in pixel area.

DISCUSSION

In Figure5, it is clear that the Ea distributions (A) [4], (B), and (C) are dominated by TAT, SRH, and Diffusion mechanisms, respectively.

Figure 6 shows that the pixels with the same dark current have various different Ea values. A long distribution tail to 1.2 [eV] at the low dark current level L1 shows diffusion component. At the middle dark current level L2, the distribution is nearly symmetric around 0.56 [eV], where SRH is dominant. At the high dark current level L3, the distribution spreads in lower than 0.56 [eV] , where TAT component is dominant.

Furthermore, Figure 7 also shows the strong correlation between dark current distributions ((i)-(iii)) and Ea distributions ((A)- (C)) although these distributions look like random. In other words, the dark current log cumulative probability plot indicates the dark current components roughly.

Finally, we demonstrate another case of the dark current log cumulative probability plot.

Figure 8 shows a comparison of the FD dark current in the different 3T_iToF. The sensor1 is the 3T_iToF discussed above. As for the sensor2, the total pixel number is 81k. The sensor2 has larger FD capacitance than the sensor1.

As shown in Figure 8(b), the sensor1 and the sensor2 are on the same trend line in spite of different total pixel number and FD layout. This fact indicates that the dark current components in these sensors are approximately the same.

Thus, the log cumulative probability plot enables us to understand the dark current characteristics easily. This plot provides a comprehensive view of dark current behavior, and it can be an effective way to compare and evaluate the characteristics of various sensors in a standardized manner.

CONCLUSION

We have revealed that the 3T_iToF has a strong correlation between Ea and dark current distribution which is followed by the TLG model. In addition, the log cumulative probability plot is very useful method to analyze devices and understand their characteristics. For the FD dark current, TAT component, which is not seen in pinned photodiode [9], causes large dark current. Thus it should be mitigated by design and process improvement.

ACKNOWLEDGEMENTS

The authors would like to thank 3T_iToF development team in Brookman Technology for their technical support, and thank DB HiTek team for the sensor fabrication.

REFERENCES

[1]. Hanh Trang, et al., "Design, implementation and evaluation of a TOF range image sensor using multi-tap lock-in pixels with cascaded charge draining and modulating gates," EIS2016

[2]. Richard L. Baer, "A model for dark current characterization and simulation," SPIE2006

[3]. Badabrata Pain, et al., "Excess Noise and Dark Current Mechanisms in CMOS imagers," IISW2005

[4]. Yamashita, et al., "Analysis of Dark Current in 4-Transistor CMOS Imager Pixel with Negative Transfer-gate bias Operation," IISW2009

[5]. Alexandre Le Roch, et al., "Leakage Current Non-Uniformity and Random Telegraph Signal in CMOS Image Sensor Floating Diffusions used for In-Pixel Charge Storage," IISW2019

[6]. M. Gurfinkel, et al., "Enhanced Gate Induced Drain Leakage Current in HfO2 MOSFETs due to Remote Interface Trap-Assisted Tunneling," IEDM2006

[7]. M. Ichikawa, et al., "Possible Models for Quasi-Composite Distributions," Reliability Engineering 8 (1984)

[8]. Ralf Widenhorn, et al., "Temperature dependence of dark current in a CCD," IISW2003

[9]. D. McGrath et al., "Dark Current Limiting Mechanisms in CMOS image Sensors," IISW2017

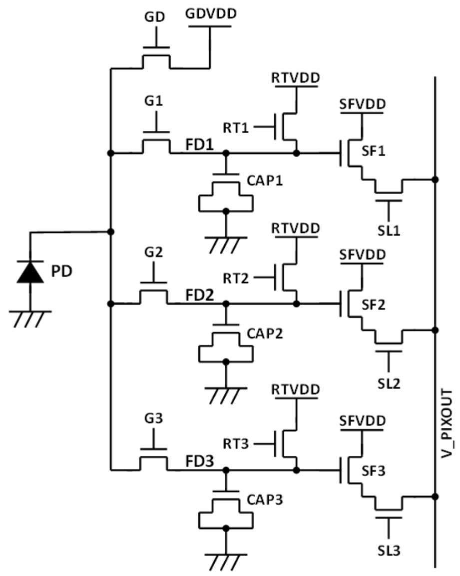

Figure 1. 3T_iToF pixel circuit

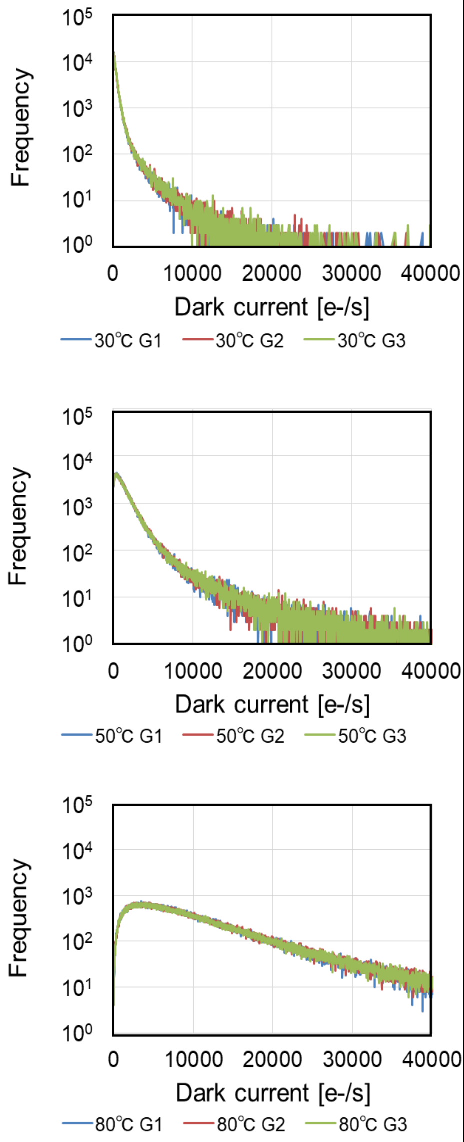

Figure 2. Dark current histogram

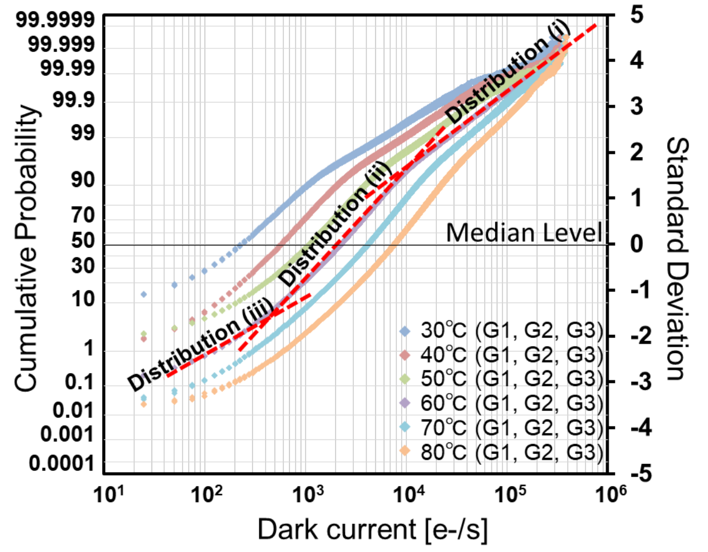

Figure 3. Dark current log cumulative probability plot

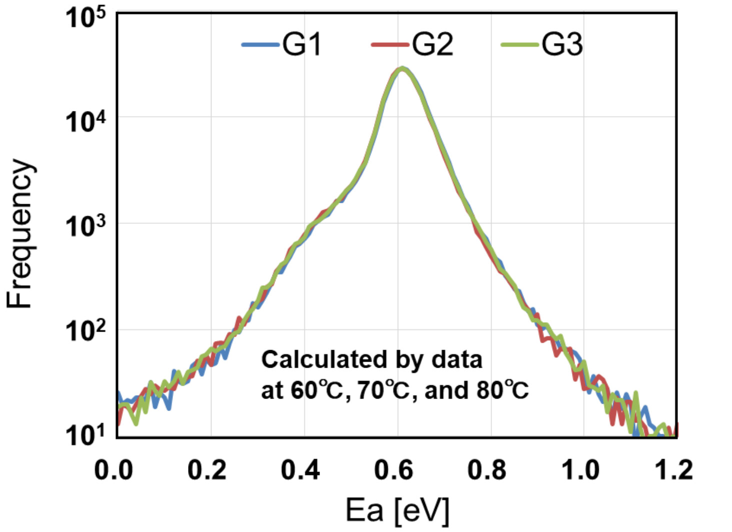

Figure 4. Ea histogram

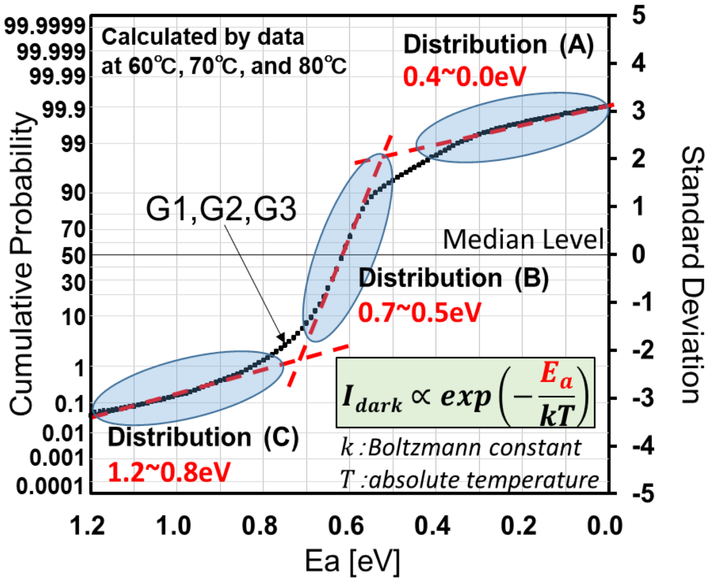

Figure 5. Ea cumulative probability plot

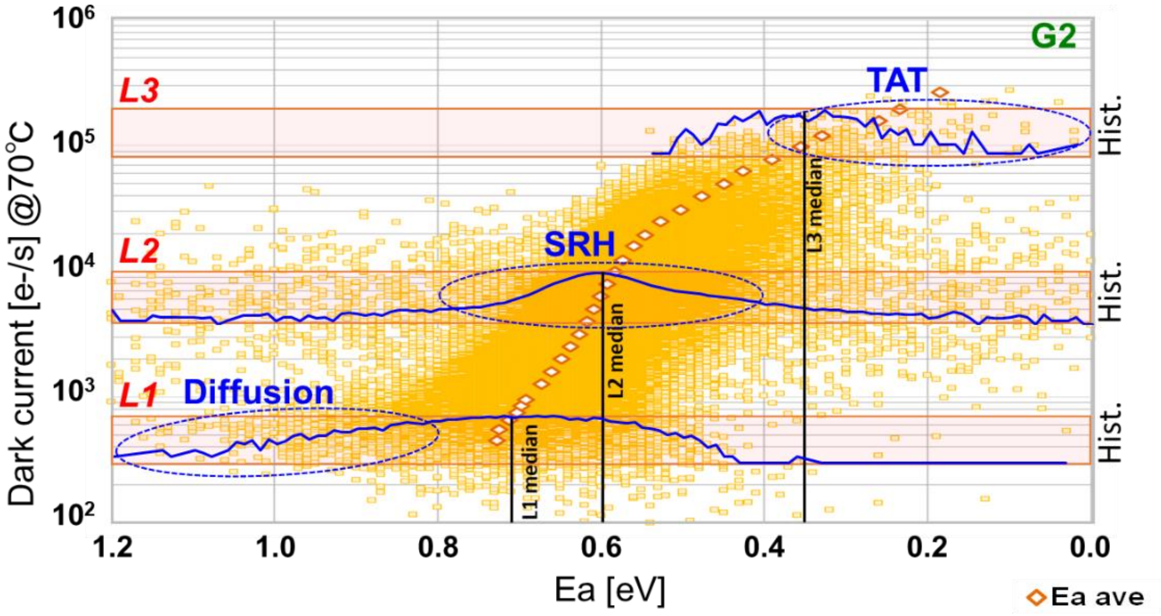

Figure 6. Scatter plot of Ea versus dark current for all pixel

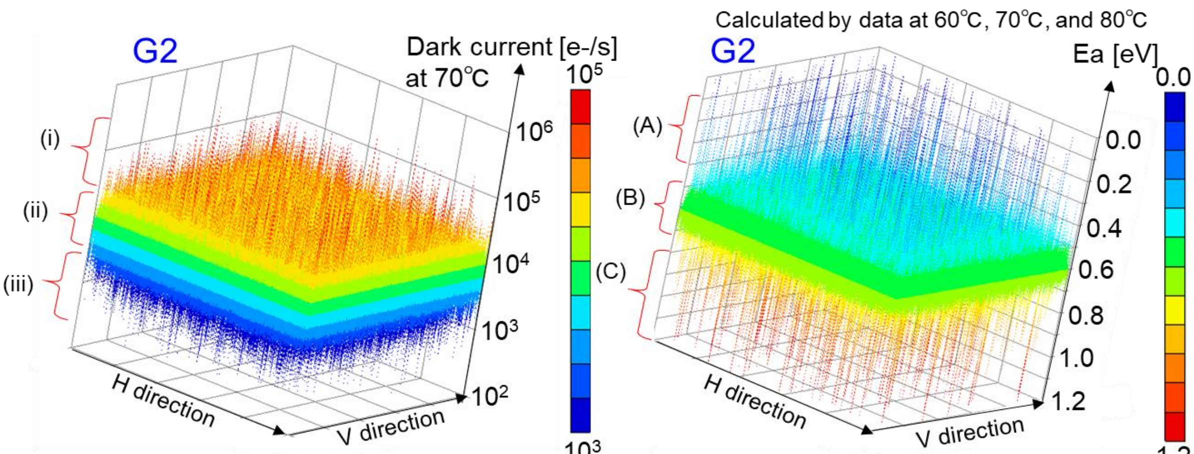

(a) 3D plot of dark current

(b) 3D plot of Ea

Figure 7. 3D plots of dark current and Ea in pixel area

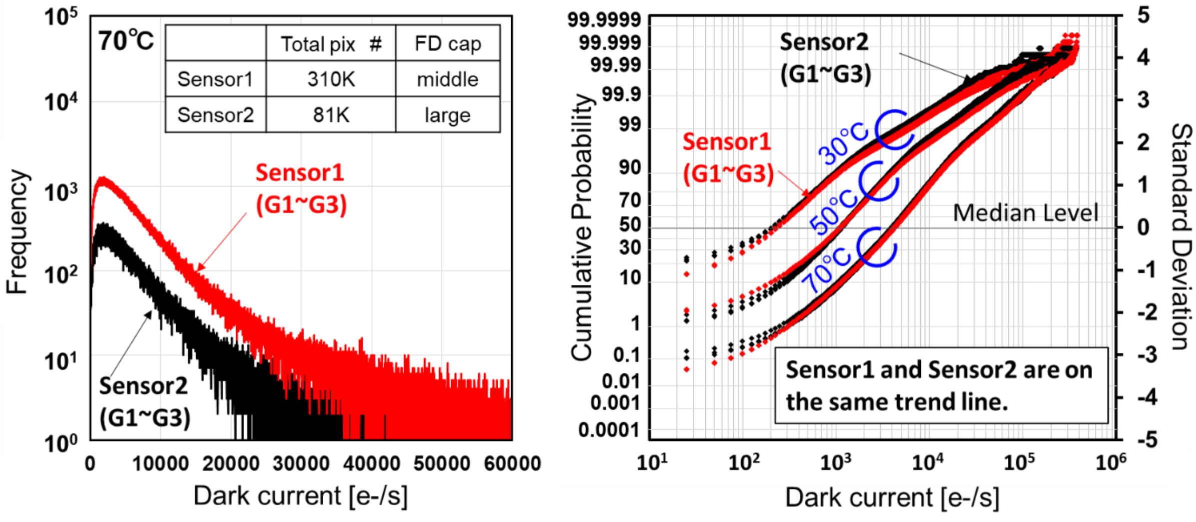

(a) histogram

(b) Cumulative probability plot

Figure 8. A comparison of FD dark current between Sensor1 and Sensor2.